ChemPubSoc Europe

DOI: 10.1002/chem.201702368

CHEMISTRY A European Journal Full Paper

Hybrid Materials

Thermosensitive Cation-Selective Mesochannels: PNIPAM-Capped Mesoporous Thin Films as Bioinspired Interfacial Architectures with Concerted Functions**

Sonja Schmidt[+],[a] Sebastián Alberti[+],[c] Philipp Vana,*[a] Galo J. A. A. Soler-Illia,[b] and Omar Azzaroni*[c]

Abstract: Rational design and elaborate modular construction of interfacial architectures in which molecular transport is mediated by responsive/adaptive nanostructures has become a growing and fertile field of research in supramolecular materials chemistry. This work presents, for the first time, the use of PNIPAM-capped mesoporous silica thin films as thermosensitive cation-selective mesochannels. Thus far, this feature has only been observed in thermosensitive biological channels. The interfacial architecture created here accomplishes its specific functions through the concerted or simultaneous action of spatially addressed subunits with temperature response and ion exclusion capabilities. The thermo-perm-selectivity effect stems from the synergistic interplay between the pH-dependent electrostatic characteristics of the silica scaffold and the thermo-controlled steric effects introduced by the capping brush layer. It is hoped that the "nanoarchitectonic" approach presented here will provide new routes toward the generation of heterosupramolecular nanosystems displaying addressable transport properties similar to those encountered in biological ion channels.

Introduction

The possibility of creating fully synthetic hybrid assemblies displaying gating and charge selectivity properties resembling those observed in biological channels is one of the grand challenges for materials science in the 21st century.[1,2] In this context, mesoporous materials have demonstrated to be a robust alternative to create nanoscopic channels as they offer exquisite control over the pore characteristics and, in addition, they are compatible with the integration into functional systems.[3–6] Part of the appeal of mesoporous nanoarchitectures is that they can incorporate chemical entities that can act as a gate and allow entry/release of chemical species into or from the mesoporous matrix.[7,8] The species can be entrapped in the inner pores or the latter can be empty. The gate opens upon application of an external stimulus and the hybrid material either releases the confined guests or permits the entrance of molecular species from the bulk solution.[9,10] During the last decade, significant research efforts have been focused on the quest for novel alternative switchable nanopore machineries capable of being "nanoactuated" by external stimuli in a controllable manner.[11,12] In this regard, one stimulus of particular interest in biological and non-biological systems is temperature.[13,14] Biological ionic channels activated by temperature changes transduce this information into conformational changes that open the channel pore. A typical example is thermosensation that is carried out by the direct activation of thermally gated ion channels in the surface membranes of sensory neurons.[15] This complex task is accomplished by temperature-sensitive cation-selective channels, which are members of the extensive TRP family (transient receptor potential channels).[16] These biological entities act as gateable ionic filters enabling the selective passage of cations only under determined thermal conditions.[17] It has been demonstrated that this gating process is achieved through the concerted functions of hydrophobic and charged residues in the biological channel.[18,19] Biological pores like TRPs pose a challenging situation that still remains elusive in molecular materials science: designing a robust, fully artificial interfacial architecture displaying charge selectivity with thermo-activated gating properties. In this context, the quest for new concepts to create novel charge-selec-

[a] *S. Schmidt,[+] Prof. P. Vana*
Georg-August-Universität Göttingen, Institut für Physikalische Chemie
Tammannstr. 6, 37077 Göttingen (Germany)
E-mail: pvana@uni-goettingen.de

[b] *Prof. G. J. A. A. Soler-Illia*
Instituto de Nanosistemas, Universidad Nacional de General San Martín
Av. 25 de Mayo 1021, San Martín, Provincia de Buenos Aires (Argentina)

[c] *S. Alberti,[+] Prof. O. Azzaroni*
Instituto de Investigaciones Fisicoquímicas Teóricas y Aplicadas (INIFTA), Departamento de Química, Facultad de Ciencias Exactas
Universidad Nacional de La Plata, CONICET, CC. 16 Suc. 4, La Plata 1900 (Argentina)
E-mail: azzaroni@inifta.unlp.edu.ar

[+] *These authors contributed equally to this work.*

[**] *PNIPAM = poly-(N-isopropylacrylamide).*

Supporting information and the ORCID identification number(s) for the author(s) of this article can be found under https://doi.org/10.1002/chem.201702368.

tive membranes is of critical importance for further expanding the scope of applications of these materials.

The integration of thermoresponsive poly-(*N*-isopropylacrylamide) (PNIPAM) in mesoporous matrices has been the subject of study of different groups.[20,21] PNIPAM is a widely studied water-soluble polymer, mainly because of its lower critical solution temperature (LCST) behavior in water, as it precipitates out from water upon heating above $T \approx 31\,^{\circ}C$.[22] This temperature-induced phase separation has been exploited for the construction of thermoassociative polymeric systems, that is, polymers that tend to associate in aqueous solution upon heating.

The first example of mesoporous materials integrating thermoactive gating properties was reported by Lopez and his collaborators in 2003.[23] These authors based their approach on the surface-initiated atom transfer radical polymerization of poly-(*N*-isopropyl acrylamide) (PNIPAM) brushes grafted from mesoporous silica particles and demonstrated that these macromolecular entities controlled the uptake and release of rhodamine 6G from the mesoporous particles. Later on, Oupicky et al.[24] showed that densely grafted PNIPAM-modified mesoporous silica nanoparticles exhibit good uptake and release properties of fluorescein at room temperature (below LCST) and a low level of leakage above LCST. According to these authors, the densely grafted PNIPAM chains constitute the capping layer that prevents the uptake and release of cargo molecules when polymer brushes are collapsed on the nanopore outlets. Since then, different groups explored similar concepts to thermally control the transport of chemical species through mesoporous matrices. However, to the best of our knowledge, the possibility of creating thermoactuated cation-selective mesoporous platforms remains fully unexplored.

In this work, we describe the creation of a hybrid organic–inorganic assembly displaying thermo-dependent ionic transport properties that, until now, were not observed in nanoporous permselective membranes. In close resemblance to TRPs, functional hybrids constituted of PNIPAM-capped mesoporous silica-based thin films are able to discriminate and modulate the transport of cations while inhibiting the passage of anions in the presence of temperature variations. Being able to design multicomponent mesoarchitectures at interfaces with functions similar to thermosensitive biological channels would be of great importance for further expanding the scope of applications of these designed nanoarchitectures.

Results and Discussion

Modification of the mesoporous films with poly-(*N*-isopropyl acrylamide) (PNIPAM) brushes was accomplished by surface-initiated reversible addition–fragmentation chain transfer (SI-RAFT) polymerization (Scheme 1). Mesoporous silica thin films were prepared through a one-pot sol-gel method by dip-coating of glass and indium tin oxide (ITO) substrates, following previously reported procedures.[25] Mesoporous films with ~200 nm thickness displaying organized pore arrays with high accessibility were obtained (Figure 1). Synchrotron-based small-angle X-ray scattering (SAXS) characterization performed at the D10A-XRD2 beamline of Laboratório Nacional de Lus Síncrotron (LNLS-Brazil) confirmed that highly organized mesopore arrays presenting a cubic $Im\bar{3}m$ mesostructure with an interpore distance of ~12 nm were obtained (Figure 1). Mesopo-

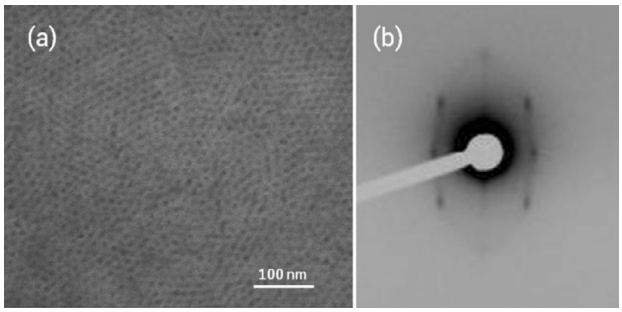

Figure 1. SEM image: a) and SAXS-2D pattern, b) of as-obtained mesoporous silica films.

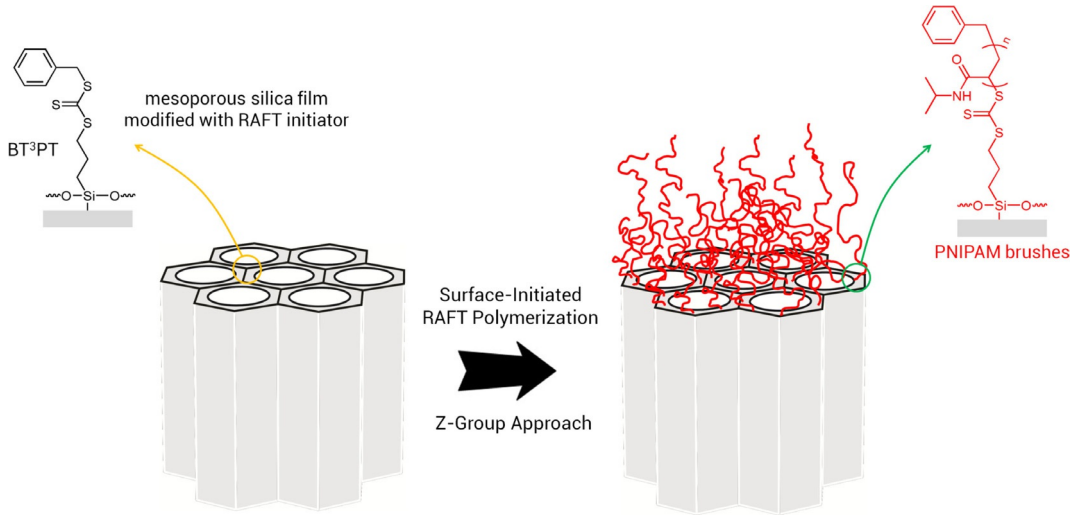

Scheme 1. Functionalization of the mesoporous silica thin film with SI-RAFT.

rous surfaces were subsequently derivatized with a RAFT agent, benzyl-(3-(trimethoxysilyl)-propyl)-trithiocarbonate (BT^3PT). Due to the hydrophobic nature of the RAFT agent, the water contact angle of the mesoporous films increased from 45° to 61° after derivatization. Then, polymer brush growth took place via SI-RAFT in the presence of the adequate solvent, monomers, and precursors (see the Supporting Information for details). This process led to the surface modification of the mesoporous film with covalently anchored PNIPAM brushes (Scheme 1). After polymerization, ellipso-porosimetry revealed only slight changes in pore and neck sizes, thus indicating that brush growth did not proceed to a large extent into the mesopores (Figure 2). However, XPS characterization of these samples indicated the appearance of an intense peak at around 399.7 eV (typical binding energy of N 1s photoelectrons), corroborating the presence of amide groups, namely PNIPAM,[26] on the mesoporous surfaces after the polymerization (Figure 3 a). Concomitantly, atomic force microscopy (AFM) imaging revealed the presence of a homogenously distributed nodular-like film grown on the mesoporous substrate and no patches or uncoated regions were found (Figure 3 b).

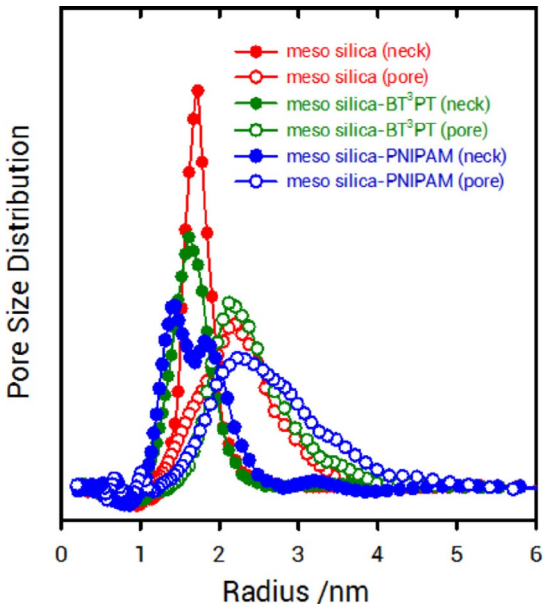

Figure 2. Pore size distribution of unmodified mesoporous silica films, mesoporous films modified with the RAFT agent (BT^3PT), and PNIPAM-modified mesoporous silica films, as determined by ellipso-porosimetry.

From these results we infer that the PNIPAM layer was grown atop the mesoporous film. From ellipsometric measurements, this polymer layer was estimated to be 9 nm in thickness. We hypothesize that the selective growth of the thermosensitive brush atop the mesoporous film originates from the steric hindrance of the chains diffusing to the surface-anchored Z-groups that precludes PNIPAM chains from entering into the mesopores. In other words, the Z-group approach can be considered as a "grafting-to" strategy as it relies on the diffusion of pre-formed polymer chains to the mesoporous surface.[27]

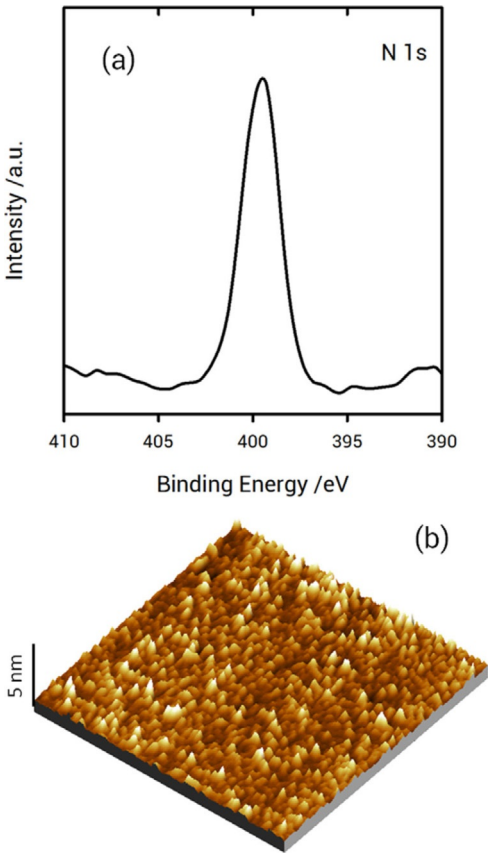

Figure 3. a) N 1s XP spectra corresponding to the mesoporous silica film after PNIPAM polymerization. b) AFM three-dimensional topography image of PNIPAM-modified mesoporous thin film (PeakForce Tapping® mode; maximum *z*-scale: 5 nm; scan size: 1.5×1.5 μm).

This fact ultimately leads to the selective tailoring of the "outer" chemistry of the hybrid mesostructured assembly (Scheme 1). This is another example of the importance of managing charge matching and steric effects between the monomer and the mesopore surface in the design of mesopore-polymer nanosystems. In previous work, the combination of cationic monomers and silanolate surfaces leads to partial to complete pore filling through monomer pre-concentration and preferential polymerization within the mesopores.[28,29] The use of a monomer containing a weak acid phosphate group partially hydrolyzed led instead to polymerization within the pores and on top of the film surface.[30]

Once we corroborated the formation of PNIPAM-capped mesoporous films, we proceeded to study the thermo-dependent permselective properties of the mesostructured hybrid interface. To this end, we characterized the transport using redox probes that diffuse across the mesoporous film deposited on a conductive ITO substrate.

Figure 4 a displays the cyclic voltammograms of PNIPAM-capped mesoporous silica films supported on ITO in the presence of 1 mM $Ru(NH_3)_6^{3+}$ and $Fe(CN)_6^{3-}$ at 20 °C, respectively. A strong inhibition in the electrochemical signal of $Ru(NH_3)_6^{3+}$ ions was observed, whereas no signal corresponding to $Fe(CN)_6^{3-}$ ions was electrochemically detected. As suggested

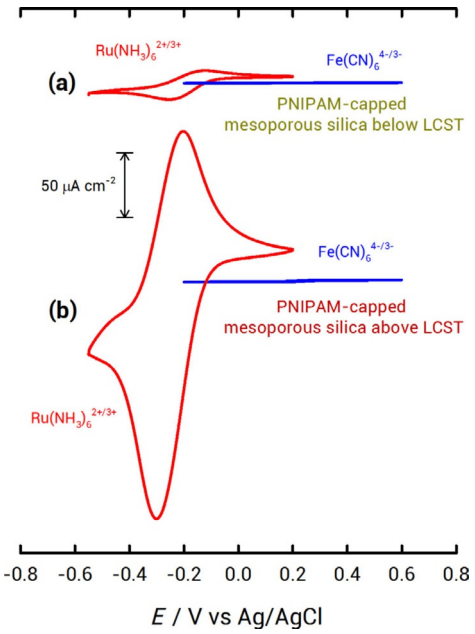

Figure 4. Cyclic voltammograms corresponding to: a) PNIPAM-modified mesoporous silica thin film at 20 °C (below LCST), b) PNIPAM-modified mesoporous silica thin film at 50 °C (above LCST), in the presence of 1 mM $Ru(NH_3)_6^{3+}$ (red trace) and 1 mM $Fe(CN)_6^{3-}$ (blue trace), respectively. Scan rate: 100 mV s^{-1}. Supporting electrolyte: 0.1 M KCl.

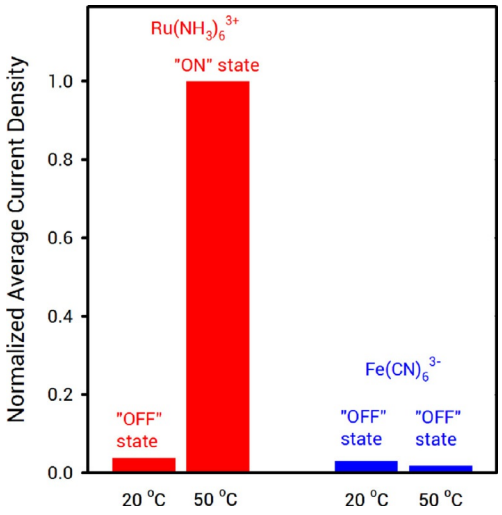

Figure 5. Histograms showing normalized variations in electrochemical current densities ("ON" and "OFF" states) arising from the influence of temperature on the molecular transport of $Ru(NH_3)_6^{3+}$ and $Fe(CN)_6^{3-}$ redox probes through the PNIPAM-modified mesoporous silica films.

by López and co-workers, below LCST the swollen PNIPAM chains can act as an effective steric barrier and block the transport through the pore openings, which is transduced by a strong decrease in the electrochemical signals of the redox probes.

Then, we set the working temperature above LCST and characterized the transport of both redox probes. Contrary to what was observed at 20 °C, upon increasing the temperature above LCST the electrochemical response of $Ru(NH_3)_6^{3+}$ strongly increased, leading to a well-defined voltammetric signal, whereas the signal corresponding to $Fe(CN)_6^{3-}$ remains fully inhibited, namely: cation-selective "ON" state. According to the mechanism demonstrated by López and collaborators, above LCST the collapsed PNIPAM chains unblock the pores, thus allowing the passage/diffusion of species from the solution into the mesopore.

In our case, the experimental data imply that the mesoporous film equipped with collapsed PNIPAM chains on the pore outlets is acting as a very efficient permselective nanostructured barrier inhibiting the transport of anionic species. It is evident that the thermoactuation of the PNIPAM layer is transduced into drastic changes in the transport properties of the mesoporous film owing to the electrostatic nature of the inner environment of the mesopore matrix. The presence of surface-confined silanolate groups (SiO^-), is responsible for conferring permselective properties to the film at pH values above the silica surface p*K*a ≈ 2.[28] The exposed SiO^- groups act as electrostatic barriers precluding the transport of anionic species. As a result, the uncapped pores operate as silanolate-gated cation-selective mesochannels; they repel the transport of $Fe(CN)_6^{3-}$ but facilitate the free diffusion of $Ru(NH_3)_6^{3+}$ ions across the inner environment of the mesoporous film.

For the sake of clarity, Figure 5 displays the histograms that reflect the relative changes in ionic transport properties under different temperature conditions for both probes. Considering that EP confirmed that mesopores are not significantly occluded with polymer, it is plausible to ascribe the strong decrease in electrochemical signals to the presence of the steric barrier arising from the swollen PNIPAM brushes sitting atop the mesoporous film. Above LCST, PNIPAM chains collapse onto the pore outlets with the concomitant unblocking of the mesopores (Scheme 2).

Furthermore, the reversibility of this nanogating process was corroborated by cycling the temperature above/below LCST. Figure 6 presents the reversible variation of the normalized electrochemical current of $Ru(NH_3)_6^{3+}$ ions in the presence of consecutive temperature changes between 20 and 50 °C. These measurements confirm the excellent transport reversibility of the thermosensitive cation-selective mesochannels.

To the best of our knowledge, this is the first experimental report on thermo-activated permselectivity in mesoporous thin films using concerted functions inside and outside the mesoporous matrix. This singular feature arises from the synergistic combination of the electrostatic characteristics of the silica scaffold and thermo-controlled steric effects introduced by the capping brush layer. Or, in other words, the unique transport properties of the hybrid interfacial could be observed only in the presence of the cooperative interaction between the "gating" of the PNIPAM layer and the anion entry exclusion exerted by the mesoporous silica surface. In most examples referring to the use of mesoporous silica in delivery systems, nanoporous matrices are relegated to mere scaffolds to create nanoscopic channels. Here, however, we described the first ex-

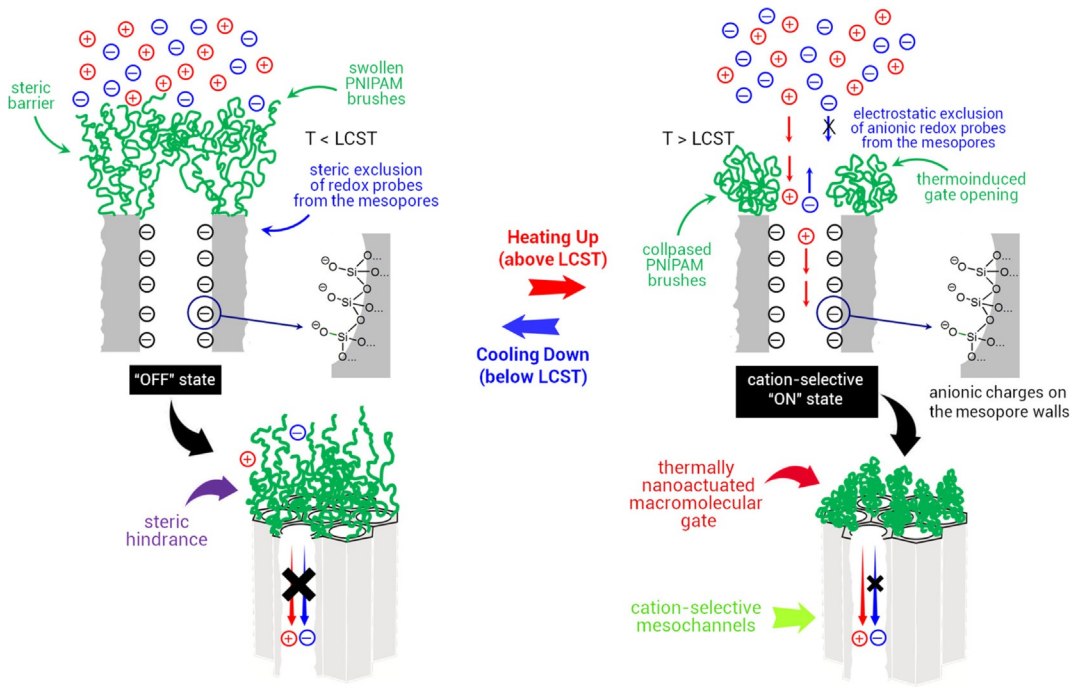

Scheme 2. Schematic depiction of the ionic transport processes taking place in the hybrid polymer-inorganic interfacial assembly at temperatures below and above LCST.

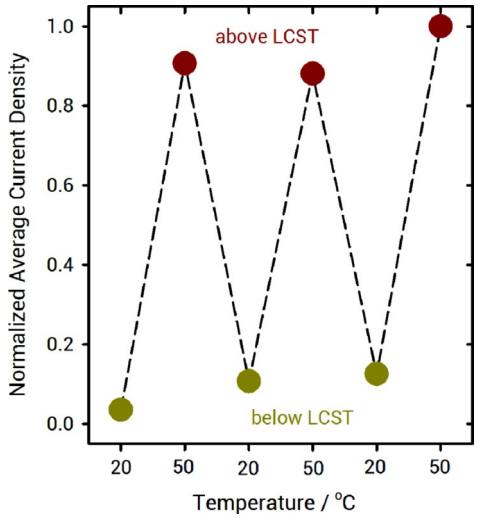

Figure 6. Reversible variation of the normalized electrochemical current of cationic $Ru(NH_3)_6^{3+}$ redox probes diffusing through PNIPAM-modified mesoporous silica films upon alternating the solution temperature between 50 °C (dark-red circles, "ON" state: above LCST) and 20 °C (dark-yellow circles, "OFF" state: below LCST). Supporting electrolyte: 0.1 M KCl.

ample in which the interplay between the intrinsic acid–base properties of the mesoporous silica scaffold and the thermo-responsive characteristics of the PNIPAM layer leads to a functional assembly with ionic transport properties so far believed to be distinctive features of biological thermo-sensing ion channels.

Conclusions

In summary, in this work we described the use of PNIPAM-capped mesoporous silica films as thermosensitive cation-selective mesochannels, a feature that has, until now, only been observed in thermosensitive biological channels. An important outcome of this research is the creation of interfacial architectures capable of accomplishing specific functions through the concerted or simultaneous action of different spatially addressed pre-designed subunits. We consider that these results may open up new avenues for producing tailored interfacial architectures displaying spatially-addressed functions, this being an emerging concept often referred to as "nanoarchitectonics".[31] This may ultimately lead to "heterosupramolecular" nanosystems with novel molecular transport functions arising from concerted interactions between inorganic and macromolecular counterparts.

Experimental Section

N-Isopropylacrylamide (NIPAM, TCI-Chemicals, 97%) and 2,2′-azobis-(methylpropionitrile) (AIBN, Akzo Nobel, 98%) were recrystallized twice from toluene/hexane (3:1) and methanol and dried. All other chemicals were obtained commercially and used without further purification. Benzyl (3-(trimethoxysilyl)-propyl)-trithiocarbonate (BT3PT) was synthesized following a procedure published earlier.[32] Ultrapure water (18 $M\Omega\,cm^{-1}$) was used in all the experiments.

Mesoporous film preparation

Synthesis of mesoporous silica thin films was performed as described in previous works,[33] by processing an ethanolic solution

containing the oxide precursor tetraethoxysilane (TEOS) in the presence of the template (F127 block copolymer, Aldrich, M = 13600). The precursor solution was prepared using 0.8 TEOS:0.2 F127:40 EtOH:10 H2O:0.28 HCl molar ratios. This solution was used to prepare the mesoporous films by dip-coating on glass and ITO substrates under ~40% relative humidity conditions at ambient temperature and 3 mm s^{-1} withdrawing speed. The organic template was removed by calcination at 350 °C for 2 h.

Surface modification with RAFT agent

The surface modification of the mesoporous silica films with RAFT agent BT3PT was accomplished by following the procedure reported by Huebner et al. with minor changes.[34] Plasma-cleaned mesoporous thin films were immersed in a solution constituted of BT3PT (0.03 mmol) and 1,2-dimethoxyethane (3 mL). The mixture was gently shaken for one day at room temperature. Then, the mesoporous thin films were washed three times with acetone and dried under a stream of nitrogen.

Polymerization procedure

A stock solution of NIPAM (2.5 g, 22 mmol, see Scheme 1), the respective RAFT agent (0.053 mmol), and 2,2-azobis-(2-methylpropionitrile) (1.7 mg, 0.011 mmol) in 1,2-dimethoxyethane (7.4 mL) was prepared and degassed using three freeze-pump-thaw cycles. Silica thin films were added under an inert atmosphere and covered with the stock solution. The samples were then conducted into a preheated oil bath of 60 °C and left for 36 h. The polymerization was stopped by cooling the samples at 0 °C and exposure to air. Subsequently, the silica thin films were washed three times with acetone and dried under a nitrogen stream. The polymerization solution was precipitated into cold diethyl ether and the resulting polymer was collected by centrifugation. The polymer was redissolved in a small amount of acetone, precipitated again in diethyl ether and centrifuged. The process was repeated once. The isolated polymers were dried in a vacuum oven at 45 °C.

Characterization

Film thickness and refractive index in the 200–950 nm region were obtained using a SOPRA GES5A spectroscopic ellipsometer. Measurement of the ellipsometric parameters θ (Theta) and Δ (Delta) were carried out under dry nitrogen flux in order to avoid water condensation within the mesopores. The film refractive index was satisfactorily adjusted according to a one-layer model for both RAFT agent functionalized and the polymer-modified mesoporous films. A Brüggemann effective medium approximation (BEMA) was used to calculate the pore volume fraction (V_{pore}/%), considering two phases made up of silica ($n_{633} = 1.455$) and void pores. The polymer volume fraction in the material V_{PNIPAM}\% was obtained by analyzing the optical data with a three component BEMA using $n_{633} = 1.455$ for the silica framework, $n_{633} = 1.50$ for PNIPAM and void pores. Water adsorption–desorption curves (at 298 K) were measured by ellipsometric porosimetry (EP, Winelli software, SOPRA Inc.). Film thickness and refractive index values were obtained from measuring the ellipsometric parameters θ (Theta) and Δ (Delta) under nitrogen flux containing controlled water vapor quantities; P/P_0 was varied from 0 to 1 (P_0 being the saturation water vapor at 298 K). Film pore volume and pore size distribution at each P/P_0 were obtained by modeling the refractive index obtained according to a three-medium BEMA (see above) corresponding to a one layer model for the mesoporous films.

Cyclic voltammetry (CV) was performed using a Gamry potentiostat with an Ag/AgCl reference electrode. All probe solutions were prepared with a concentration of 1 mM in 100 mM KCl as supporting electrolyte resulting in a pH 5–6 solution. Quantitative variations in permselectivity were studied by following the changes of voltammetric peak currents associated to cationic $Ru(NH_3)_6]^{2+/3+}$ and anionic $[Fe(CN)_6]^{4-/3-}$ redox probes, diffusing across the mesoporous film.

Atomic force microscopy (AFM) measurements were performed on a Multimode AFM (Bruker) with a NanoScope V controller using PeakForce Tapping™ with a TAP525 A Cantilever (Bruker, nominal spring constant: 200 N m^{-1}, nominal resonance frequency: 525 kHz, nominal radius 8 nm) in argon at room temperature. All images were taken with a scan rate of 0.977 Hz, and a resolution of 512 × 512 samples per line. For the analysis of the data the program Gwyddion was used.

Size exclusion chromatography (SEC) characterization of all samples was performed with DMAc containing 0.1% (by mass) of lithium bromide as the eluent using an Agilent 1260 Infinity system. It was composed of an autosampler, an isocratic solvent pump, a PSS GRAM (polyester copolymer network) precolumn (8 × 50 mm), three PSS GRAM separation columns (8 × 300 mm, nominal particle size = 10^{-5} m; pore sizes = 30, 103, and 103 Å) maintained at 45 °C in a column compartment, an 80 Hz UV detector (set to a wavelength of 310 nm for the RAFT polymers), and a refractive index (RI) detector. The flow rate of the mobile phase was 8×10^{-4} L min^{-1}. The whole setup was calibrated with a total of 12 PSS poly-(methyl methacrylate) standards ($M_n = 0.8$–1820 kg mol^{-1}) of low dispersity with toluene as internal standard. All samples were filtered through a 450 nm PTFE syringe filter prior to injection. The concentration of the polymer samples was 3 g L^{-1}.

Dynamic light scattering (DLS) measurements were conducted on a Zetasizer Nano S (Malvern) with a laser ($\lambda = 633$ nm) by using 12 mm quartz cuvettes. Intensity distributions were recorded with 12 runs of a run duration of 20 s per measurements. All measurements were recorded under a detection angle of 173°.

Contact angle (CA) was measured with an OCA 15EC (OCA Measuring Instruments) using the TBO Video based contact angle measuring system by Dataphysics. A water drop (2 μL) was placed at five different spots on the surfaces. The presented results are an average of the five measurements.

Scanning electron microscopy (SEM) images were obtained with a ZEISS LEO GEMINI field emission electron microscope (CMA, Facultad de Ciencias Exactas y Naturales, UBA, Argentina).

Acknowledgements

S.S. acknowledges financial support by the Deutsche Forschungsgemeinschaft, DFG (project-nr. VA226/9). S.A. acknowledges a doctoral scholarship from CONICET. G.J.A.A.S.I. and O.A. are CONICET fellows and acknowledge financial support from Fundación Petruzza, CONICET (PIP 0370) and ANPCYT (PICT-2012-2087, PICT-2013-0905, PICT 2014–3687, PICT 2015–3526). Financial support provided by the DFG-CONICET German-Argentinian Collaborative Program in Physical Chemistry (MU 1674#15-1) is also recognized and gratefully acknowledged.

Conflict of interest

The authors declare no conflict of interest.

Keywords: mesoporous materials · PNIPAM · polymer brushes · responsive materials · thin films

[1] a) B. V. V. S. P. Kumar, K. V. Rao, S. Sampath, S. J. George, M. Eswaramoorthy, *Angew. Chem. Int. Ed.* **2014**, *53*, 13073 – 13077; *Angew. Chem.* **2014**, *126*, 13289 – 13293; b) *Nanobiotechnology of Biomimetic Membranes* (Ed.: D. Martin), Wiley, New York, **2007**; c) S. Alberti, G. J. A. A. Soler-Illia, O. Azzaroni, *Chem. Commun.* **2015**, *51*, 6050 – 6075; d) R. Lehner, X. Wang, M. Wolf, P. Hunziker, *J. Controlled Release* **2012**, *161*, 307 – 316.

[2] M. Tagliazucchi, in *Chemically Modified Nanopores and Nanochannels* (Eds.: M. Tagliazucchi, I. Szleifer), Elsevier, Oxford, **2017**, pp. 1 – 19;

[3] a) G. J. A. A. Soler-Illia, O. Azzaroni, *Chem. Soc. Rev.* **2011**, *40*, 1107 – 1150; b) A. Vinu, K. Z. Hossain, K. Ariga, *J. Nanosci. Nanotechnol.* **2005**, *5*, 347 – 371.

[4] Q. Ji, S. Acharya, J. P. Hill, A. Vinu, S. B. Yoon, J.-S. Yu, K. Sakamoto, K. Ariga, *Adv. Funct. Mater.* **2009**, *19*, 1792 – 1799.

[5] I. I. Slowing, B. G. Trewyn, V. S.-Y. Lin, in *The Supramolecular Chemistry of Organic – Inorganic Hybrid Materials* (Eds.: K. Rurack, R. Martínez-Mañez), Wiley, Hoboken, **2010**, p. 479.

[6] C. Sanchez, C. Boissiere, S. Cassaignon, C. Chaneac, O. Durupthy, M. Faustini, D. Grosso, C. Laberty-Robert, L. Nicole, D. Portehault, F. Ribot, L. Rozes, C. Sassoye, *Chem. Mater.* **2014**, *26*, 221 – 238.

[7] a) C. Coll, A. Bernardos, R. Martínez-Mañez, F. Sancenón, *Acc. Chem. Res.* **2013**, *46*, 339 – 349; b) P. Yang, S. Gai, J. Lin, *Chem. Soc. Rev.* **2012**, *41*, 3679 – 3698; c) Q. He, J. Shi, *J. Mater. Chem.* **2011**, *21*, 5845 – 5855; d) D. Tarn, C. E. Ashley, M. Xue, E. C. Carnes, J. I. Zink, J. Brinker, *Acc. Chem. Res.* **2013**, *46*, 792 – 801.

[8] a) Z. Li, J. C. Barnes, A. Bosoy, J. F. Stoddart, J. I. Zink, *Chem. Soc. Rev.* **2012**, *41*, 2590 – 2605; b) L. Minati, V. Antonini, M. Dalla Serra, G. Speranza, F. Enrichi, P. Riello, *Microporous Mesoporous Materials* **2013**, *180*, 86 – 91; c) M. Yu, S. Jambhrunkar, P. Thorn, J. Chen, W. Gu, C. Yu, *Nanoscale* **2013**, *5*, 178 – 183; d) X. Wan, G. Zhang, S. Liu, *Macromol. Rapid Commun.* **2011**, *32*, 1082 – 1089; e) F. Tang, L. Li, D. Chen, *Adv. Mater.* **2012**, *24*, 1504 – 1534.

[9] a) M. Hecht, E. Climent, M. Biyikal, F. Sancenón, R. Martínez-Máñez, K. Rurack, *Coord. Chem. Rev.* **2013**, *257*, 2589 – 2606; b) A. Brunsen, J. Cui, M. Ceolín, A. del Campo, G. J. A. A. Soler-Illia, O. Azzaroni, *Chem. Commun.* **2012**, *48*, 1422 – 1424; c) A. Calvo, B. Yameen, F. J. Williams, O. Azzaroni, G. J. A. A. Soler-Illia, *Chem. Commun.* **2009**, 2553 – 2555; d) A. Brunsen, C. Díaz, L. I. Pietrasanta, B. Yameen, M. Ceolín, G. J. A. A. Soler-Illia, O. Azzaroni, *Langmuir* **2012**, *28*, 3583 – 3592.

[10] a) S. Angelos, E. Johansson, J. F. Stoddart, J. I. Zink, *Adv. Funct. Mater.* **2007**, *17*, 2261 – 2271; b) M. W. Ambrogio, C. R. Thomas, Y.-L. Zhao, J. I. Zink, J. F. Stoddart, *Acc. Chem. Res.* **2011**, *44*, 903 – 913; c) L. Du, S. Liao, H. A. Khatib, J. F. Stoddart, J. I. Zink, *J. Am. Chem. Soc.* **2009**, *131*, 15136 – 15142.

[11] a) X. Hou, H. Zhang, L. Jiang, *Angew. Chem. Int. Ed.* **2012**, *51*, 5296 – 5307; *Angew. Chem.* **2012**, *124*, 5390 – 5401; b) X. Hou, W. Guo, L. Jiang, *Chem. Soc. Rev.* **2011**, *40*, 2385 – 2401.

[12] a) E. Aznar, C. Coll, M. D. Marcos, R. Martínez-Máñez, F. Sancenón, J. Soto, P. Amorós, J. Cano, E. Ruiz, *Chem. Eur. J.* **2009**, *15*, 6877 – 6888; b) A. Agostini, F. Sancenón, R. Martínez-Máñez, M. D. Marcos, J. Soto, P. Amorós, *Chem. Eur. J.* **2012**, *18*, 12218 – 12221; c) R. Mortera, J. Vivero-Escoto, I. I. Slowing, E. Garrone, B. Onida, V. S.-Y. Lin, *Chem. Commun.* **2009**, 3219–3221. d) Y. Zhao, J. L. Vivero-Escoto, I. I. Slowing, B. G. Trewyn, V. S.-Y. Lin, *Expert Opin. Drug Delivery* **2010**, *7*, 1013–1029.e) E. Climent, R. Martínez-Máñez, F. Sancenón, M. D. Marcos, J. Soto, A. Maquieira, P. Amorós, *Angew. Chem. Int. Ed.* **2010**, *49*, 7281–7283; *Angew. Chem.* **2010**, *122*, 7439–7441. f) E. Aznar, L. Mondragón, J. V. Ros-Lis, F. Sancenón, M. D. Marcos, R. Martínez-Máñez, J. Soto, E. Pérez-Payá, P. Amorós, *Angew. Chem. Int. Ed.* **2011**, *50*, 11172 – 11175; *Angew. Chem.* **2011**, *123*, 11368 – 11371.

[13] a) D. W. Urry, *Angew. Chem. Int. Ed. Engl.* **1993**, *32*, 819; *Angew. Chem.* **1993**, *105*, 859; b) H. Nakatsuji, T. Numata, N. Morone, S. Kaneko, Y. Mori, H. Imahori, T. Murakami, *Angew. Chem. Int. Ed.* **2015**, *54*, 11725 – 11729; *Angew. Chem.* **2015**, *127*, 11891 – 11895.

[14] a) B. Yameen, M. Ali, R. Neumann, W. Ensinger, W. Knoll, O. Azzaroni, *Small* **2009**, *5*, 1287 – 1291; b) W. Guo, H. Xia, F. Xia, X. Hou, L. Cao, L. Wang, J. Xue, G. Zhang, Y. Song, D. Zhu, Y. Wang, L. Jiang, *ChemPhysChem* **2010**, *11*, 859 – 864.

[15] J. Huang, X. Zhang, P. A. McNaughton, *Semin. Cell Dev. Biol.* **2006**, *17*, 638.

[16] R. Latorre, S. Brauchi, G. Orta, C. Zaelzer, G. Vargas, *Cell Calcium* **2007**, *42*, 427.

[17] H. Xu, I. S. Ramsey, S. A. Kotecha, M. M. Moran, J. A. Chong, D. Lawson, P. Ge, J. Lilly, I. Silos-Santiago, Y. Xie, P. S. DiStefano, R. Curtis, D. E. Clapham, *Nature* **2002**, *418*, 181 – 186.

[18] M.-F. Tsai, C. Miller, *Cell* **2014**, *158*, 977 – 979.

[19] S. Chowdhury, B. W. Jarecki, B. Chanda, *Cell* **2014**, *158*, 1148 – 1158.

[20] a) K. Murakami, S. Watanabe, T. Kato, K. Sugawara, *Colloids Surf. A* **2013**, *419*, 223 – 227; b) M. Bathfield, J. Reboul, T. Cacciaguerra, P. Lacroix-Desmazes, C. Gerardin, *Chem. Mater.* **2016**, *28*, 3374 – 3384; c) P.-W. Chung, R. Kumar, M. Pruski, V. S.-Y. Lin, *Adv. Funct. Mater.* **2008**, *18*, 1390 – 1398.

[21] a) A. De Sousa, D. Andrada Maria, R. G. De Sousa, E. M. Barros de Sousa, *J. Mater. Sci.* **2010**, *45*, 1478 – 1486; b) J.-H. Park, Y.-H. Lee, S.-G. Oh, *Macromol. Chem. Phys.* **2007**, *208*, 2419 – 2427; c) M. M. Russell, L. Raboin, T. M. Guardado-Alvarez, J. I. Zink, *J. Sol-Gel Sci. Technol.* **2014**, *70*, 278 – 285.

[22] a) H. G. Schild, *Prog. Polym. Sci.* **1992**, *17*, 163 – 249; b) A. Baeza, E. Guisasola, E. Ruiz-Hernández, M. Vallet-Regí, *Chem. Mater.* **2012**, *24*, 517 – 524.

[23] a) Q. Fu, G. V. R. Rao, L. K. Ista, Y. Wu, B. P. Andrzejewski, L. A. Sklar, T. L. Ward, G. P. Lopez, *Adv. Mater.* **2003**, *15*, 1262 – 1266; b) Q. Fu, G. V. Rama Rao, T. L. Ward, Y. Lu, G. P. Lopez, *Langmuir* **2007**, *23*, 170 – 174.

[24] Y.-Z. You, K. K. Kalebaila, S. L. Brock, D. Oupicky, *Chem. Mater.* **2008**, *20*, 3354 – 3359.

[25] a) A. Calvo, P. C. Angelomé, V. M. Sánchez, D. A. Scherlis, F. J. Williams, G. J. A. A. Soler-Illia, *Chem. Mater.* **2008**, *20*, 4661; b) G. J. A. A. Soler-Illia, C. Sanchez, B. Lebeau, J. Patarin, *Chem. Rev.* **2002**, *102*, 4093; c) G. J. A. A. Soler-Illia, P. Innocenzi, *Chem. Eur. J.* **2006**, *12*, 4478.

[26] S. Won, D. J. Phillips, M. Walker, M. I. Gibson, *J. Mater. Chem. B* **2016**, *4*, 5673 – 5682.

[27] J. Moraes, K. Ohno, T. Maschmeyer, S. Perrier, *Chem. Commun.* **2013**, *49*, 9077 – 9088.

[28] A. Andrieu-Brunsen, S. Micoureau, M. Tagliazucchi, I. Szleifer, O. Azzaroni, G. J. A. A. Soler-Illia, *Chem. Mater.* **2015**, *27*, 808 – 821.

[29] M. Rafti, A. Brunsen, M. C. Fuertes, O. Azzaroni, G. J. A. A. Soler-Illia, *ACS Appl. Mater. Interfaces* **2013**, *5*, 8833 – 8840.

[30] Ref. [9d].

[31] a) K. Ariga, M. Li, G. J. Richards, J. P. Hill, *J. Nanosci. Nanotechnol.* **2011**, *11*, 1 – 13; b) K. Ariga, Q. Ji, J. P. Hill, Y. Bando, M. Aono, *NPG Asia Mater.* **2012**, *4*, e17 – 11; c) K. Ariga, Q. Ji, W. Nakanishi, J. P. Hill, M. Aono, *Mater. Horiz.* **2015**, *2*, 406 – 413.

[32] R. Rotzoll, D. H. Nguyen, P. Vana, *Macromol. Symp.* **2009**, *275 – 276*, 1 – 12.

[33] P. Angelomé, G. J. A. A. Soler-Illia, *J. Mater. Chem.* **2005**, *15*, 3903 – 3912.

[34] D. Huebner, V. Koch, B. Ebeling, J. Mechau, J. E. Steinhoff, P. Vana, *J. Polym. Sci. Part A* **2015**, *53*, 103 – 113.

Manuscript received: May 23, 2017

Accepted manuscript online: August 10, 2017

Version of record online: September 12, 2017